

Top quark as a gate to new physics: Z' production in top events at an e^+e^- collider

Ambroise Espargilière

LAPP, Annecy, France

Laboratoire d'Annecy le Vieux de Physique des Particules (LAPP)

CNRS : UMR5814 - IN2P3 - Université de Savoie

E-mail: ambroise.espargiliere@lapp.in2p3.fr

Abstract. In Randall-Sundrum theories a dark matter candidate can arise consequently to baryon number conservation in the form of a massive right handed Dirac neutrino interacting through an additional $SU(2)_R$ gauge group. The neutral $SU(2)_R$ gauge boson, called Z' , is supposed to couple only to the standard model right handed top quark. In e^+e^- collisions it will therefore be produced preferentially in top events. Its production is studied in the channel $e^+e^- \rightarrow t\bar{t}Z'$ and a method to measure its mass is proposed. The generator level measurement shows a precision better than 10% for a light Z' ($m_{Z'} \in [200, 500]$ GeV).

1. Introduction

Many theories have been built to fill in the Standard Model (SM) deficiencies (super-symmetry, Kalusa-Klein, ...). The so-called Grand Unified Theories (GUTs) have to cope with many questions to be relevant. The dark matter puzzle is one of those. Dark matter is constituted of yet unknown massive particles. Such particles accounts for the major part of the galaxy masses and can be detected thanks to gravitational effects (galaxy dynamics, gravitational lensing). Dark matter accounts as well for $\approx 25\%$ of the universe energy budget. In many GUTs, a dark matter particle candidate arises as a spin-off of the baryon number conservation (*e.g.* the neutralino being stabilised thanks to the R-parity in super symmetry). In the case of Randall-Sundrum theories, the baryon number conservation leads to the stability of a particle having the properties of a right handed neutrino ν' [1, 2]. This ν' interact *via* an additional $SU(2)_R$ gauge group involving, among others, a neutral gauge boson called Z' .

The expected main properties of this new particles (details in [3] and [4]) are the following:

- Small coupling to the SM through a Z^0/Z' mixing at the percent level. Too high mixing would conflict with direct dark matter detection constraints.
- Z' couples to the SM only *via* right handed top quark t_R .
- The Z' mass $m_{Z'}$ must be in the TeV range but as light as possible.
- The ν' mass $m_{\nu'}$ must be a bit below $m_{Z'}/2$ to comply with the relic density constraints.

As a consequence, this Z' can not be directly produced in e^+e^- collisions in a resonant process such as $e^+e^- \rightarrow Z'$ and the benefit must be taken from its strong coupling to the top quark. In the next section, the Z' production in e^+e^- collisions is described and the choice of the studied Z' decay channel is discussed. In section 3 the selection of the events showing a Z' is drawn and

in section 4 the cross section of the production process is measured using the event selection method and a technique for the measurement of the Z' mass $m_{Z'}$ is proposed. The analysis is done at the generator level. Data are generated using the software calcHEP 2.5.5 [5] and pythia 8 [6] is used to propagate and decay the particles. Some inputs from a full detector simulation are considered in section 4.3.

2. Z' production in 3 TeV e^+e^- collisions

Since the Z' is supposed to couple in the SM mainly (or uniquely) to the top quark, a favoured production process in e^+e^- collisions is the emission by an out-going $t\bar{t}$ pair. The corresponding diagram is displayed in figure 1.

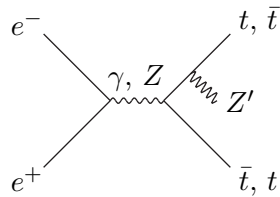


Figure 1. Z' production by emission from an out-going $t\bar{t}$ pair.

In the present set-up, if the small Z^0/Z' mixing is neglected, two decay channels are possible for the Z' : the decay into a $t\bar{t}$ pair, allowed if its mass is sufficient, and the decay into $\nu'\bar{\nu}'$ pair, always allowed since the ν' has been taken at a mass below $m_{Z'}/2$.

Recent LHC results (elsewhere in those proceedings) have shown that a leptophobic Z' , that would show up as a resonance in di-jet mass or $t\bar{t}$ pair invariant mass spectra, are very unlikely for Z' masses below ≈ 1.5 TeV. On the other hand, in the process discussed above, if the Z' decayed into a $t\bar{t}$ pair, a four top event would be obtained, giving therefore a striking signal at a 3 TeV e^+e^- collider (the SM cross section for four top events is ≈ 20 ab). The study is therefore focused on the invisible decay of a light Z' ($200 \text{ GeV} \leq m_{Z'} < 1 \text{ TeV}$) after emission by an out-going $t\bar{t}$ pair produced in a 3 TeV e^+e^- collision. The cross sections of this process for different mass of the Z' are shown in table 1 at a centre of mass energy of 3 TeV and includes the effect of Initial State Radiations (ISR).

Table 1. Total process cross sections and Z' decay branching ratios times cross section.

$m_{Z'}$	Cross sect.	$\sigma_{Z' \rightarrow \text{inv.}}$	$\sigma_{Z' \rightarrow t\bar{t}}$
200 GeV/ c^2	14.9 fb	14.9 fb	—
300 GeV/ c^2	8.7 fb	8.7 fb	—
400 GeV/ c^2	5.6 fb	2.4 fb	3.2 fb
500 GeV/ c^2	3.7 fb	1.2 fb	2.5 fb
600 GeV/ c^2	2.6 fb	0.8 fb	1.8 fb
700 GeV/ c^2	1.8 fb	0.5 fb	1.3 fb

3. Z' event selection

The main characteristics of signal and backgrounds are summarised below. A method to discriminate the signal events is proposed.

3.1. Signal and background characteristics

The signal consists of multi-jet events with a large number of particles and a certain amount of missing energy. It is expected to be very close to SM s -channel $t\bar{t}$ events which constitute the main background. In a first step, the tagging of the top events is assumed to have a full efficiency and purity. Therefore, the backgrounds considered are only the SM inclusive $t\bar{t}$ events and the following background channels are leftover for this study (cross sections given at 3 TeV for boson hadronic decays only):

- $e^+e^- \rightarrow W^+W^-$ (263 fb)
- $e^+e^- \rightarrow Z^0Z^0$ (16 fb)
- $e^+e^- \rightarrow W^+W^-Z^0$ (11 fb)
- $e^+e^- \rightarrow Z^0Z^0Z^0$ (< 1 fb)

The present results shall then be scaled according to the real top tagging performance.

Both s and t channel $t\bar{t}$ production are considered, their respective Feynman diagrams are displayed in figure ?? (note that, for background 2, only the main diagram is represented) and their respective cross sections are summed up in table 2.

(i) background 1: $e^+e^- \rightarrow t\bar{t}$ (ii) background 2: $e^+e^- \rightarrow t\bar{t} + \nu\bar{\nu}$

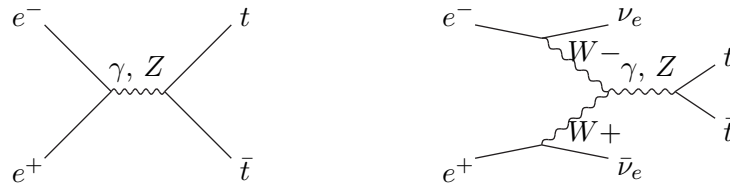


Figure 2. Diagrams of the considered background channels

Table 2. background channel cross sections.

Channel	Cross sect.
$e^+e^- \rightarrow t\bar{t}$	19.87 fb
$e^+e^- \rightarrow t\bar{t} + \nu\bar{\nu}$	5 fb

3.2. Selection results

The event selection is performed with a cut on the output of a Boosted Decision Tree (BDT) evaluated for each event. The discriminative input variables are listed in table A1. They are all related to the event dynamics, event shape and to missing energy. The BDT output distributions for signal and background is displayed on figure 3 and the performance of the separation are summarised in table 3. S_{\max} denote the maximum significance and therefore corresponds to the optimal cut. The global efficiency of the event selection is 0.884 ± 0.004 .

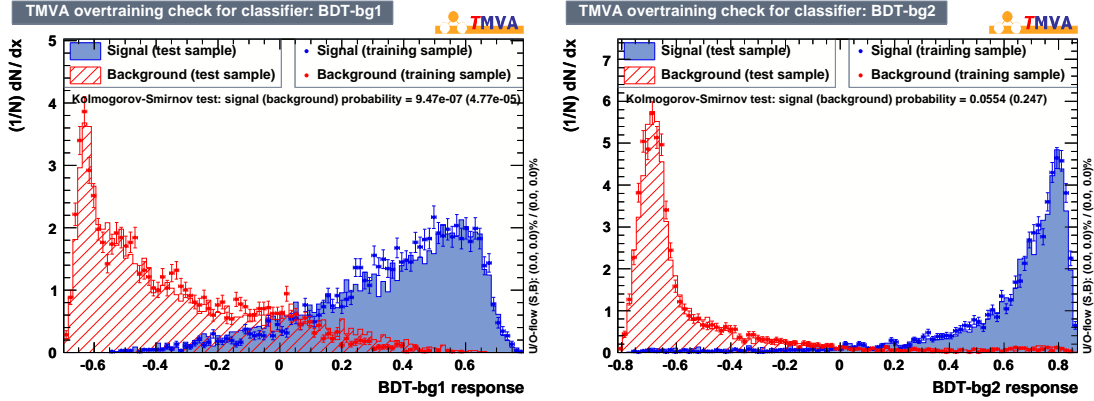


Figure 3. BDT output distributions for signal and both backgrounds.

Table 3. BDT performance.

	Sig. vs Bg1	Sig. vs Bg2	\mathcal{P}_T cut
\int ROC	0.955	0.971	N/A
S_{\max}	99.6	113.8	88.6
$\epsilon@S_{\max}$	90.8%	97.4%	85%
$B@S_{\max}$	18.0%	14.6%	40.3%
S_{\max} cut	-0.0378	-0.3391	175 GeV/c

4. Measurement of process cross section and Z' mass

4.1. Method for Z' mass measurement

The Z' mass can be extracted from the event total invariant mass spectrum (or equivalently from the $t\bar{t}$ pair invariant mass) of the selected events. In absence of Z' and without any source of smearing, this spectrum should simply show a thin peak at the nominal energy of the collisions. In the case of the emission of a Z' by the out-going $t\bar{t}$ pair, the energy transferred to the Z' becomes invisible. The Z' tends to be emitted at rest or very low energy, therefore the invariant mass spectrum should show a peak at the nominal collision energy minus the Z' mass and a tail towards lower values. Nevertheless, the ISR induces a smearing of the collision energy, as shown in figure 4. It therefore induces a smearing of the spectrum and then a smoothing of the spectrum upper edge. A function, called “smooth gate” in the following, defined in eq. 1, is fitted to the event total invariant mass spectrum without presence of the signal as shown in figure 5(c). This way the background contribution is modeled and is subtracted from the total spectrum. The area of the remaining spectrum is then proportional to the cross section of the $e^+e^- \rightarrow t\bar{t}Z'$ process. To measure the Z' mass, the “smooth gate” is fitted to this spectrum as shown in figure 5(d) and the s_2 parameter, corresponding to the upper slope inflexion point, is related to $m_{Z'}$ through the relation 3 established in the following. The “smooth gate” is defined by:

$$f(x) = \frac{A}{(e^{\frac{s_1-x}{p_1}} + 1)(e^{\frac{x-s_2}{p_2}} + 1)}, \quad (1)$$

where s_i , $i \in \{1, 2\}$ are the inflection point abscissae and p_i , $i \in \{1, 2\}$ are the slope steepnesses, see graphical representation with arbitrary values of the parameters in figure 5(b).

The procedure described above is applied for $m_{Z'}$ from 200 to 700 GeV/ c^2 with a constant

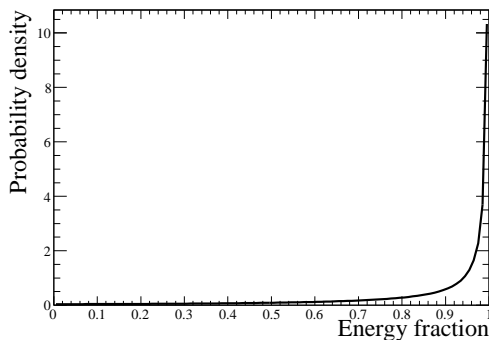


Figure 4. Distribution of the fraction of nominal collision energy due to ISR.

statistics. The use of a constant statistics is meant to probe the s_2 sensitivity to $m_{Z'}$ only. The resulting event invariant mass spectra are displayed in figure 5(e). Their fitted “smooth gate” upper inflexion point abscissa are summed up in table 4 and plotted in figure 5(f). This figure shows as well how a straight line fits to the data point and the residuals are shown in the figure corner histogram. The fit information allows to define a relation between the s_2 parameter and $m_{Z'}$ which reads:

$$s_2 = (2757 \pm 8) - (1.05 \pm 0.02) \times m_{Z'}, \quad (2)$$

which gives a direct formula for $m_{Z'}$:

$$m_{Z'} = \frac{(2757 \pm 8) - s_2}{1.05 \pm 0.02}. \quad (3)$$

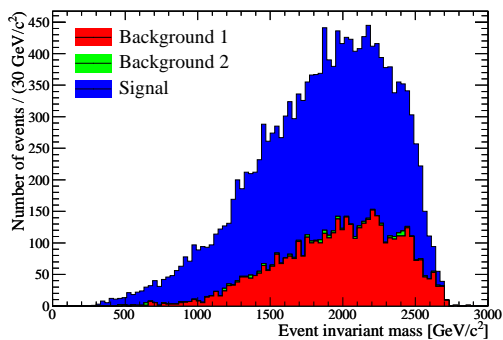
Table 4. Summary of the “smooth gate” upper inflexion point abscissae (s_2)

$m_{Z'}$ (GeV/ c^2)	s_2 (GeV/ c^2)
200	2530 ± 6
300	2458 ± 6
400	2340 ± 7
500	2235 ± 7
600	2119 ± 8
700	2005 ± 10

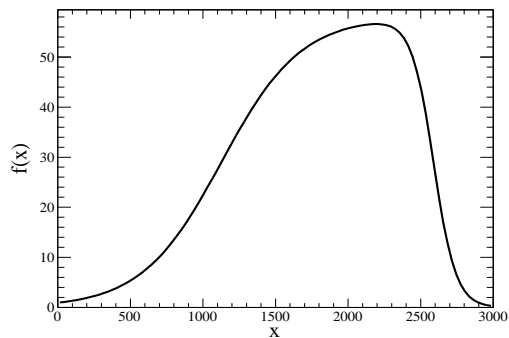
4.2. Results with model predicted

The model predicted statistics for 1 ab^{-1} of data are used in order to estimate the cross section measurement and the expected resolution on $m_{Z'}$.

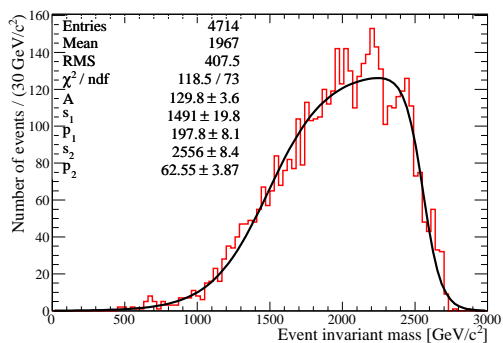
4.2.1. Event selection and cross section measurement Table 5 summarizes the main features of the analysis using the model predicted statistics: for each mass, the table shows the number of events passing the BDT cuts and surviving the background subtraction and the significance of the new physics signal. The measured cross sections are shown as well and compared to the predicted ones. The present method tend to underestimate the process cross section for low $m_{Z'}$ and slightly over-estimate it at higher values.



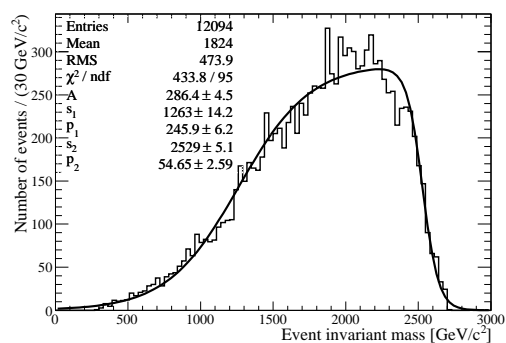
(a) Event total invariant mass spectrum for signal and both backgrounds ($m_{Z'} = 200 \text{ GeV}/c^2$).



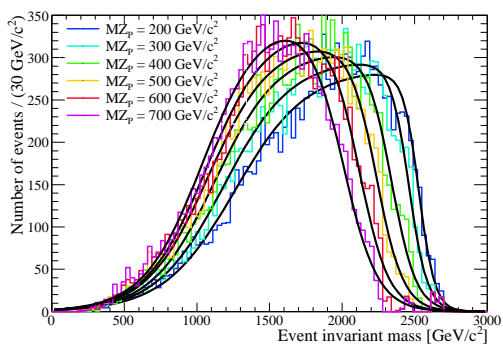
(b) “Smooth gate” function with arbitrary parameter values.



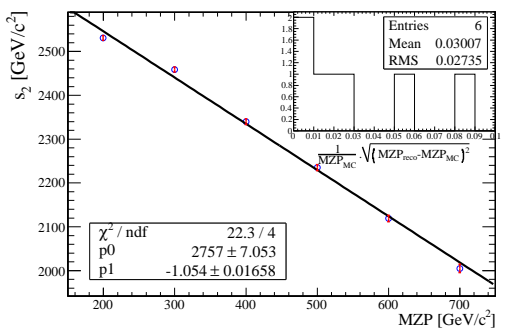
(c) Event total invariant mass spectrum after event selection, for background only, fitted with the “smooth gate” function.



(d) Event total invariant mass spectrum after event selection and background subtraction fitted with the “smooth gate” function for $m_{Z'} = 200 \text{ GeV}/c^2$.



(e) Event total invariant mass spectrum after event selection and background subtraction fitted with the “smooth gate” function for various Z' masses.



(f) s_2 parameter versus $m_{Z'}$.

Table 5. Z' events using model predicted statistics and cross section measurement results

$m_{Z'}$	Events yield	Significance	True cross sect.	Measured cross sect. (fb)
200	12094	92.7	14.9 fb	13.7 ± 0.2
300	7411	66.6	8.7 fb	8.4 ± 0.1
400	2150	24.6	2.4 fb	2.4 ± 0.04
500	1192	13.5	1.2 fb	1.3 ± 0.02
600	815	8.4	0.8 fb	0.9 ± 0.02
700	642	5.6	0.5 fb	0.7 ± 0.02

4.2.2. Z' mass measurement and expected resolution Table 6 summarizes the value of the s_2 parameter with its error for each Z' mass and the corresponding measured mass deduced from relation 3. It appears here that above $m_{Z'} = 500 \text{ GeV}/c^2$ the event yield is not sufficient to perform a reliable fit and the s_2 returned values do not make sense, thus the Z' mass would not be measurable. For $m_{Z'}$ between 200 and 500 GeV/c^2 the mass can be measured with a precision better than 10%.

Thanks to eq. 3, it is now possible to predict the Z' mass from a $t\bar{t}$ event invariant mass spectrum to which a “smooth gate” function is fitted (see definition in eq. 1). As $m_{Z'} = (k - s_2)/\alpha$, the error margin on this prediction reads:

$$\begin{aligned} \Delta m_{Z'} &= \underbrace{\frac{\Delta k}{\alpha}}_{\text{constant term}} \oplus \underbrace{\frac{m_{Z'} \Delta \alpha}{\alpha}}_{\text{linear term}} \oplus \underbrace{\frac{\Delta s_2}{\alpha}}_{\text{fit term}}. \quad (4) \\ &= 7.8 \text{ GeV}/c^2 \oplus 0.95 \Delta s_2 \oplus 1.9\% m_{Z'} \end{aligned}$$

The errors Δk and $\Delta \alpha$ are inherent to the measurement method itself. Hence, the constant and the linear term of eq. 4 describe systematic uncertainties. They may be reduced by refining the analysis on the s_2 dependency on $m_{Z'}$. For instance, using more statistics for each value of $m_{Z'}$ and/or using more values of $m_{Z'}$ are possible refinements. Whereas the error Δs_2 comes from the event invariant mass spectra fitted with the “smooth gate” function and can only be improved by the accumulation of more statistics. Thus, the so-called “fit term” reflects the statistical uncertainty on $m_{Z'}$. The precise resolution is predicted using eq. 4 and values from table 5 and 6. The result is plotted in figure 5.

Table 6. Z' mass measurement results

$m_{Z'} (\text{GeV}/c^2)$	$s_2 (\text{GeV}/c^2)$	Measured $m_{Z'} (\text{GeV}/c^2)$
200	2529 ± 6	217 ± 11
300	2448 ± 8	294 ± 13
400	2342 ± 20	395 ± 22
500	2282 ± 40	454 ± 40
600	913 ± 82	1756 ± 86
700	962 ± 78	1710 ± 82

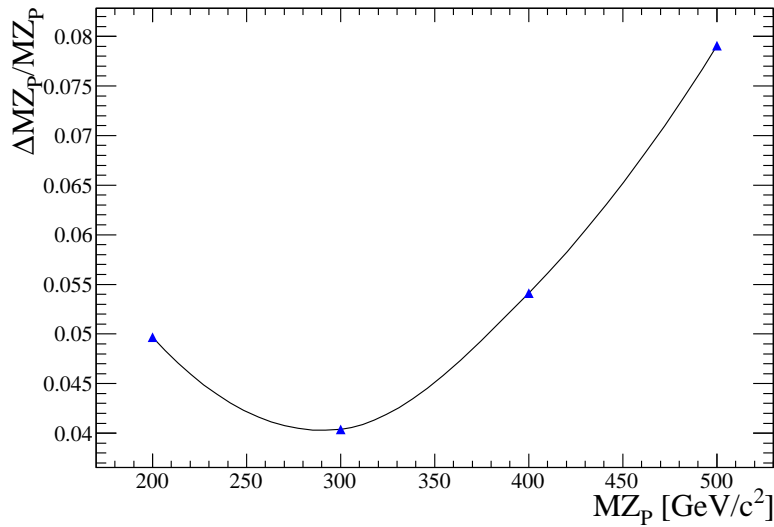


Figure 5. $m_{Z'}$ error vs. $m_{Z'}$.

4.3. Inputs from full simulation

The full simulation has been performed in the framework of the preparation of CLIC CDR [7]. The detector model is the CLIC version of the ILD detector. CLIC beamstrahlung has been simulated in details and the $\gamma\gamma \rightarrow hadrons$ machine background (≈ 3 interaction per bunch crossing) has been included. Pandora PFA [8] has been used for data reconstruction.

Standard Model data sample have been available to evaluate the detector resolution on the variables and test top tagging performance. Figure 6 focuses on the resolution on the event total invariant mass and illustrate the fact that this variable is not robust against the finite detector resolution and the machine background. So far, the event total invariant mass was similar to the $t\bar{t}$ pair invariant mass which is the key variable for the $m_{Z'}$ measurement, therefore, a careful reconstruction of the top quarks four-vector will allow a reliable calculation of the $t\bar{t}$ pair invariant mass. The selection of boosted hadronic top events is an example of strategy to perform a precise reconstruction of top quark four-vector without messing up with problems of missing energy.

In figure 7, the separation between s -channel $t\bar{t}$ events and inclusive hadronic $W^+ W^-$ events is illustrated. A boosted decision tree is used as well. The preliminary performance sketched here indicate that $t\bar{t}$ events may be rather well extracted and that no dramatic degradation of the results presented is expected.

5. Conclusion

The Dark Matter candidate emerging from Randall-Sundrum theories (and possibly others) has the quantum numbers of a right handed Dirac neutrino ν' . This neutrino interacts *via* an additional gauge group $SU(2)_R$ as a right handed analogy with weak interaction. A Z' boson, being the neutral gauge boson of $SU(2)_R$, couples only to the right handed top quark in the Standard Model and therefore can be produced in e^+e^- collision only *via* emission by an out-going $t\bar{t}$ pair.

This Z' , if too light, can only decay into $\nu'\bar{\nu}'$ and avoids the present day LHC exclusions of a Z' resonance decaying into $t\bar{t}$ pairs. In this case the Z' can be discovered in $t\bar{t}$ event samples and its mass can be measured with a precision better than 10% with 1 ab^{-1} of data. The analysis has been carried out at the generator level, preliminary results from full simulation indicates that

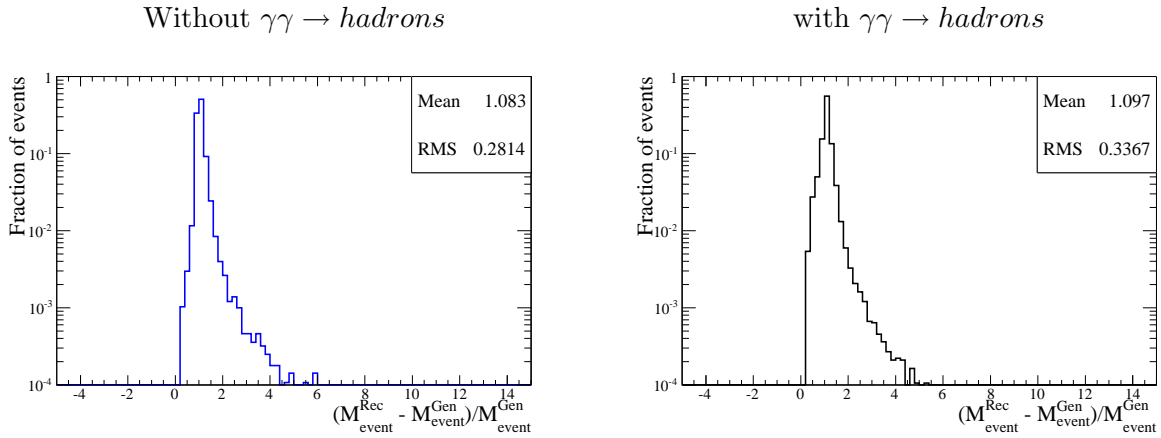


Figure 6. Resolution on the event total invariant mass after full simulation.

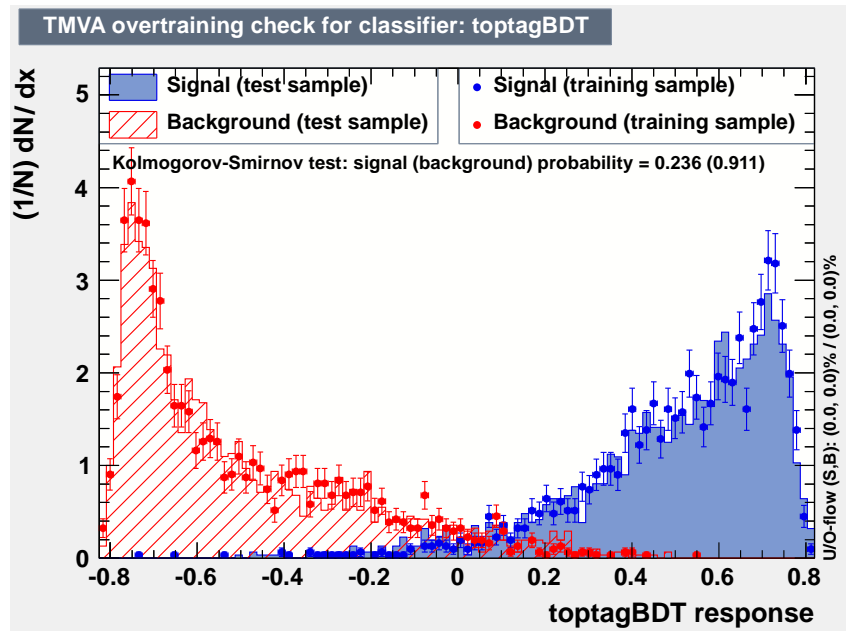


Figure 7. Separation between $t\bar{t}$ and $W^+ W^-$ events.

the total event invariant mass is not robust against a finite detector resolution and a special care must be given to a precise reconstruction of the top quarks four-vectors (*e.g.* selecting boosted hadronic tops) and the $t\bar{t}$ pair invariant mass will replace the event invariant mass in the analysis. The top tagging performance seems promising and no critical degradation of those results is expected. a complementary note on the generator level study can be found in [9].

Acknowledgement

The first acknowledgement goes to the conference organisers for giving me the opportunity to present this work. The author would like to thank Geneviève Bélanger, Marco Battaglia and Géraldine Servant for their help in guiding this study at the beginning (the choice of the channel, the model parameter values to use...). Many thanks as well for Sasha Pukhov and Geneviève Bélanger again, for answering all my questions about the RHNM and calcHEP and to Peter

Skands for helping me fix the interface between calcHEP and Pythia8. The author would like especially to thank Jean-Jacques Blaising for advices, useful discussions and precious help.

Appendix A. BDT input variables

Table A1. Summary of the analysis variables

Variable name	Description	Discriminating power
missPT	Missing transverse momentum	3.462e-01
missE	Missing energy	3.114e-01
jet1E	First hemisph. energy	3.012e-01
jet2E	Second hemisph. energy	2.496e-01
jet2P	Second hemisph. momentum	2.365e-01
missP	Missing momentum	2.250e-01
jet1P	First hemisph. momentum	2.138e-01
jetPTdiff:=jet1P-jet2P	hemisph. PT difference	2.122e-01
missA	Angle of missing momentum	1.134e-01
jet2PT	Second hemisph. transverse momentum	1.078e-01
sphericity	Sphericity	1.024e-01
aplanarity	Aplanarity	9.443e-02
jetEratio:=jet2E/jet1E	Hemisph. energy ratio	9.302e-02
Jet1PT	First hemisph. transverse momentum	7.763e-02
jetEdiff:=jet1E-jet2E	Hemisph. energy difference	6.089e-02

References

- [1] Agashe K and Servant G 2004 *Phys. Rev. Lett.* **93** 231805
- [2] Agashe K and Servant G 2005 *J. Cosmol. Astropart. Phys.* JCAP02(2005)002 (*Preprint hep-ph/0411254*)
- [3] Bélanger G, Pukhov A and Servant G 2008 *J. Cosmol. Astropart. Phys.* JCAP01(2008)009 (*Preprint 0706.0526 [hep-ph]*)
- [4] Jackson C B *et al* 2010 *J. Cosmol. Astropart. Phys.* JCAP04(2010)004 (*Preprint 0912.0004 [hep-ph]*)
- [5] Pukhov A 2004 *Preprint hep-ph/0412191*
- [6] PYTHIA 8 home page: <http://home.thep.lu.se/~torbjorn/Pythia.html>
- [7] CLIC collaboration: <http://clic-study.org>
- [8] Thomson M 2009 *Nucl. Instrum. Meth. A* **611** 25–40 (*Preprint arXiv:0907.3577 [physics.ins-det]*)
- [9] Espargilière A 2011 *to be released*